Experimental Characterization and Mechanical Behavior Analysis on Intermetallic Compounds of 96.5Sn-3.5Ag and 63Sn-37Pb Solder Bump with Ti-Cu-Ni UBM on Copper Chip

Chih-Tang Peng[1], Chia-Tai Kuo[1], Kuo-Ning Chiang[2],
E-Mail: Knchiang@pme.nthu.edu.tw
Department of Power Mechanical Engineering
National Tsing Hua University
HsinChu, Taiwan 300, R.O.C.

Terry Ku[3], Kenny Chang[3]
VIA Technology Corporation

Abstract

Due to today's trend towards 'green' products, the environmentally conscious manufacturer is moving toward lead-free schemes for electronic devices and components. Nowadays the bumping process has become a branch of the infrastructure of flip chip bonding technology. However, the formation of excessively brittle intermetallic compounds between under bump metallurgy (UBM)/solder bump interface influences the strength of solder bumps within flip chips, and may create a package reliability issue. Based on the above reason, this study investigated the mechanical behavior of lead-free solder bumps affected by the solder/UBM intermetallic compounds formation in the duration of isothermal aging. To attain the objective, the test vehicles of Sn-Ag (lead-free) and Sn-Pb (lead-containing) solder bump systems designed in different solder volumes as well as UBM diameters were used to experimentally characterize and analyze their mechanical behavior. It is worth to mention that, to study the intermetallic compound growth mechanism and the mechanical behavior of a electroplated solder bump on a Ti/Cu/Ni UBM layer fabricated upon a copper chip, the test vehicles are compose of, from bottom to top, the copper metal pad on silicon substrate, a Ti/Cu/Ni UBM layer and electroplated solder bumps. By way of metallurgical microscope and scanning electron microscopy (SEM) observation**,** the interfacial microstructure of test vehicles were measured and analyzed. In addition, a bump shear test is utilized for the strength determination of solder bumps. Different shear displacement rates were selected to study the time-dependent failure mechanism of the solder bumps. The results indicated that after isothermal aging treatment at 150^0C for over 1000 hours, the Sn-Ag solder revealed a better maintenance of bump strength than that of Sn-Pb solder, and the Sn-Pb solder showed a higher intermetallic compounds growth rate than that of Sn-Ag solder. In addition, it was concluded that the test vehicles of copper chip with the selected Titanium/Copper/Nickel UBMs showed good bump strength in both Sn-Ag and Sn-Pb systems as the intermetallic compound grows. Furthermore, the study of shear displacement rate effect on the solder bump strength indicates that the analysis of bump strength versus thermal aging time should be identified as a qualitative analysis for solder bump strength determination rather than a quantitative one. In terms of the solder bump volume and the UBM size effects, both the Sn-Ag and the Sn-Pb solders showed no significant effect to the intermetallic compounds growth rate.

Keywords:
Sn-Ag solder, Sn-Pb solder, lead-free, intermetallic compounds, UBM, and isothermal aging

I. Introduction

Flip-chip technology provides many advantages, including high I/O connections, high electrical performance, and high reliability. As a result it has attracted a great deal of attention for advanced electronic packaging applications. As a bonding material, the tin-lead solder has served as the primary material for many years. However, owing to environmental issues with the lead ingredient of the tin-lead solder, the electronic industry tends to utilize lead-free solder, leading to a gradual replacement of the tin-lead solder in the future. For these reasons, the characteristics of the lead-free solder bump, such as the influence on long-term package reliability, intermetallic compounds growth inducing bump strength variation, and the UBM selection for the bumping process, which were never fully developed, should be studied thoroughly.

Particularly in flip chip technology, both in high Pb-Sn and eutectic Sn-Pb, the solder joint are the mainstream interconnection. However, the investigation of the lead-free assemblies has been recently become intensified due to the legislation the use of lead in electronic products. Although it has been demonstrated that lead-free soldering is technologically possible and shows some advantages [1,2], there are many technical issues to be addressed before it will be fully and succesfully implemented. Sn-Ag-Cu eutectic solder is now accepted as a general-purpose baseline lead-free solder. Nevertheless, the electroplating technology today has several limitations in applying ternary composition plating to the wafer level process. First, complex alloy systems such as ternary or quaternary alloys are impractical for the solder bumping process. Solder bump placement is generally achieved by electroplating or evaporation through a metal

1. Graduate Assistant, Ph.D candidate
2. ***Corresponding Author***, Professor, Dept. of Power Mechanical Engineering, National Tsing Hua University/Electronics Research and Service Organization, Industrial Technology Research Institute, HsinChu, Taiwan
3. VIA Technology Corporation

mask. Electroplating of complex alloy systems is difficult especially when the compositional control is critical. For solders with more than three components, co-evaporation is impractical due to the limited target source allowed. Therefore, simple alloy systems are far more convenient in the flip chip solder bumping process. The relatively larger alloy content is also important for process development. If the target alloy composition is less than 1 wt.%, the composition analysis contains more uncertainty, and the process optimization becomes more difficult [3]. Among several of the lead-free solder materials, the eutectic Sn-Ag alloy system is a promising candidate [4] because it not only shows a qualified mechanical strength [2], lower melting temperature (221^{o}C), lower surface tension, better ductility, and a relatively larger alloying metal content, and a better wettability, but it also provides a fabrication possibility for the solder electroplating bumping process.

To fabricate flip chip packages with high performance, many problems such as fine pitch, uniformity, electrical reliability and production cost have to be considered. In bumping techniques, stencil printing and electroplating are widely used. The current capability of the bump pitch of electroplating process is below 50μm, which reveals a finer bump pitch than the stencil printing process (the current capability of the bump pitch of the stencil printing process is limited to 150μm). Furthermore, the electroplated bumping can provide a better uniformity for bump height and bump diameter [5]. Therefore, the electroplating method, one of a cost effective bumping process, not only provides flexibility with respect to bump size and pitch, but also has a high production throughput. Basis of above reasons, the Sn-Ag electroplating solder shows a good potential for ultra high-density application in the future.

Nowadays, Cu is considered as a promising chip interconnection material in Si-based integrated circuits due to its lower electrical resistivity and better resistance to the electromigration than that of Al alloys [6]. Critical advances over the last several years have enabled the development and implementation of copper in the semiconductor design. However, not many studies have been performed on the flip chip interconnection of copper chips. Therefore, it is necessary to investigate the effects of intermetallic compound formation upon UBM/solder strength on Cu pads during the duration of thermal aging. The UBM material selection also shows significant effects for package reliability and intermetallic compound composition [1,7]. To obtain an appropriate bumping process, the UBM and solder interface reactions should be studied and the selection of metallization, thickness, and process must be carefully considered and defined. Recently, the solder/surface finishing intermetallic compound formation mechanism has been detail studied in [1,7,8,9,10], and the effect of solder bump volume on intermetallic compound formation was also presented in [11]. However, a detailed mechanical behavior of the lead-free solder bump influenced by the intermetallic compound formation was never fully discussed.

Thermal preconditioning is used by many investigators to expose or accelerate latent defects that result in brittle interfacial fractures. There is no universal set of preconditioning test parameters, because aging and reflow do not induce the same failure mechanism. Isothermal aging generally is beneficial when devices are going to be subjected to extended high temperature storage, burn-in, or bake-out prior to transport [12,13]. Therefore, the elevated temperature isothermal aging preconditioning is adopted in this research to study the intermetallic compound growth mechanism and its influence on bump shear strength.

Based on the reasons mentioned above, this study presents a thorough study of the solder bump mechanical behavior affected by intermetallic compounds growth. The alloys fabricated by the electroplating process include 63Sn-37Pb and 96.5Sn-3.5Ag. The UBMs on the Cu metal pad include Ti/Cu and electrolytic Ni. The characteristics of the test vehicles of electroplated Sn-Ag and Sn-Pb solder systems are together compared for the performance determination of the electroplated Sn-Ag solder with Ti/Cu/Ni UBMs. The topics of discussion in this investigation include the bump strength degradation induced by intermetallic compound growth for both Sn-Ag and Sn-Pb solder systems, the solder bump volume and UBM size effect on the intermetallic compound formation, the comparison of intermetallic compound growth rate between Sn-Ag and Sn-Pb solders, the morphology and the composition of intermetallic compound layer at the Ti/Cu/Ni UBM/solder interface, the time-dependent mechanical behavior of solder bumps, and the fracture surface variety of Sn-Ag and Sn-Pb solders as the high temperature storage time increases.

II. Specimen Preparation

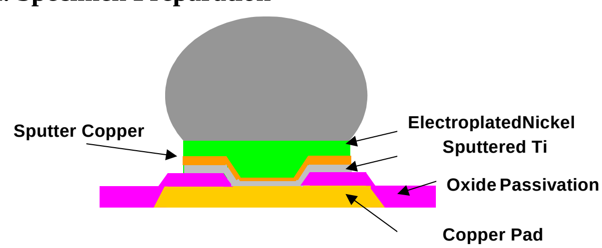

Fig. 1: Sketch of the bump structure

Figure 1 illustrates the bump structure in this research. The top metal layer of the Si wafer is Cu, which is sputtered on the wafer and acts as an interconnection line. A passivation layer is deposited and patterned on the wafer as a protection for the metal trace. The adhesion layer is sputtered Ti with a thickness at the angstrom level. Then a Cu layer with a thickness at the angstrom level is sputtered on the Ti for an electroplating seed layer. Consequently, a photolithography process is employed for the bump location patterning. Electroplated Ni with a thickness of 1 μm, which provides a good barrier to inhibit vast and detrimental growth of the Cu-Sn intermetallic compound, is then deposited on the predetermined metallized area. After the UBM layer (Ti-Cu-Ni) is plated onto the Si wafer, the 63Sn-37Pb and 96.5Sn-3.5Ag solder bump is then electroplated. All metal films are deposited consecutively. The following four metal etching processes are applied for the solder bump structure formation. Finally, the solder reflow process is conducted in a solder reflow oven. The peak temperature and the dwelling time are 220°C and 74sec for Sn-Pb solder and 250°C and 78sec for Sn-Ag solder, respectively. Figure 2 depicts the bump photographs of the Sn-Ag and Sn-Pb solders.

(a) (b)

(c) (d)

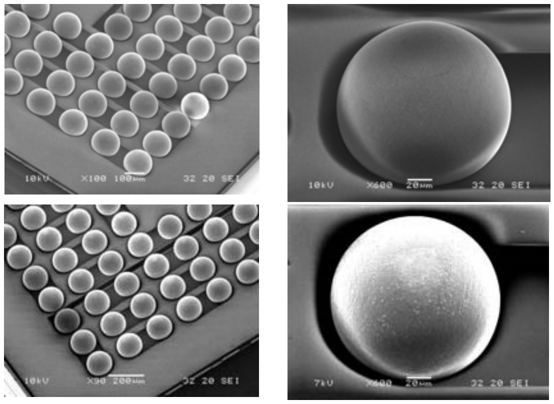

Fig. 2: The bump photographs, (a) Sn-Pb flip chip solder bumps, (b) single Sn-Pb solder bump, (c) Sn-Ag flip chip solder bumps and (d) single Sn-Ag solder bump

The chip dimension is 10.6 x 10.6 x 0.725 (mm). The bump pitch is 200μm, the distance of the outmost bump center to die edge is 400μm, and the bump count is 735. In this study, six testing vehicles: MPE005Pb, MPE006Pb, MPE007Pb, MPE005Ag, MPE006Ag and MPE007Ag are prepared. Table 1 indicates the bump specifications of these specimens.

Table 1. The specifications of the testing vehicles

Specimen	*Solder Material*	*Copper Pad Diameter (μm)*	*UBM Diameter (μm)*	*Average Bump Height (μm)*
MPE005Pb	63Sn-37Pb	125	110	87
MPE006Pb	63Sn-37Pb	135	120	91
MPE007Pb	63Sn-37Pb	145	130	93
MPE005Ag	96.5Sn-3.5Ag	125	110	84
MPE006Ag	96.5Sn-3.5Ag	135	120	85
MPE007Ag	96.5Sn-3.5Ag	145	130	88

III. Experimental Procedures

In order to study the effect of intermetallic compound formation, the isothermal aging treatment is employed as an accelerating mechanism to accelerate the intermetallic compound layer growth rate. The choice of isothermal aging rather than thermal cycling aging in this investigation is owing to the fact that the isothermal aging process shows a higher coincidence with what happens in the practical application case (high temperature storage, such as burn-in) than the thermal cycling aging process. The test vehicles are aged with isothermal treatment at 150^0C for 24, 48, 72, 96, 120, 240, 480, 720 and 1000 hours respectively. To verify how the intermetallic compounds formation influences the bump strength, the mechanical strength of the solder bumps is evaluated with a shear tester (Dage-4000) using different shear speed (10, 100 and 200μm/s) at a shear height of 8μm. The different shear speeds could assist us to study the time-dependent failure mechanism of solder bumps in relation to the growth of the intermetallic compound layer.

After isothermal aging, both the as-reflowed and heat treated samples are subjected to be molded in an epoxy resin, following the cross sectioning and polishing of the test vehicles for examination. In order to appropriately identify the thickness of the intermetallic compound layer, a wet grinding on successively finer grit abrasive papers is utilized, using from 600 grit through 2400 grit abrasives. Subsequently, the test vehicles are successively polished with 1μm diamond abrasives on a rotating polishing wheel covered with a synthetic polishing cloth. The mean thickness of the interfacial intermetallic compound layer is measured using a powerful image processing system (OPTIMAS) and a metallurgical microscope. An energy dispersive x-ray (EDX) is used to examine the morphology and the composition of the intermetallic compound layer at the UBM/solder interface. A SEM is applied to observe the microstructure details of the solder systems to investigate the relationship between the fracture mechanism and the intermetallic compound layer growth.

IV. Results and Discussion

- Effects of isothermal aging on the microstructure

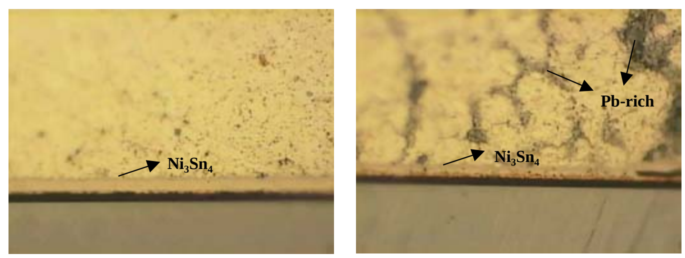

(a) (b)

Fig. 3: The interfacial morphology and composition of (a) Sn-Ag and (b) Sn-Pb systems as-reflowed

Figure 3 illustrates the interfacial morphology and composition of the Sn-Ag and Sn-Pb systems as solder reflowed. It can be observed in the figure that for the Sn-Ag and Sn-Pb systems, only a thin layer (less than 1μm) of Ni-Sn intermetallic compound phase is found at the UBM/solder interface as solder reflowed.

The energy dispersive x-ray (EDX) is applied to examine the morphology and the composition of the intermetallic compound layer at the UBM/solder interface. An HCl tin (Sn) etching is applied (as shown in figure 4) for the detailed intermetallic compound composition observation and detection. Figure 5 indicates the EDX analysis findings, and it is shown that the intermetallic compound layer composition of the Sn-Ag and Sn-Pb solder systems are Ni/Sn compounds. These compositions can be expressed as Ni_3Sn_4. Figure 6 depicts the intermetallic compound layers of test vehicles of Sn-Ag and Sn-Pb solder systems after isothermal aging. In figure 6, both of the intermetallic compounds layer thicknesses of the Sn-Ag and Sn-Pb solders elevate as the isothermal aging time increases. The detailed Ni_3Sn_4 intermetallic compound layer thickness measured by the image processing system (OPTIMAS) and the metallurgical microscope is illustrated in figure 7.

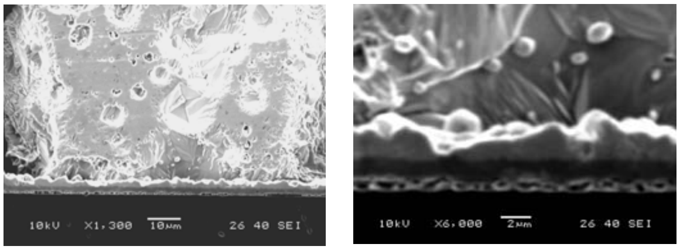

(a)

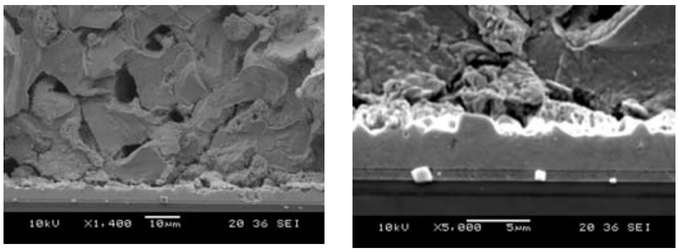

(b)

Fig. 4: A HCl tin (Sn) etching for (a) Sn/Ag solder and (b) Sn/Pb solder after 1000 hours isothermal aging

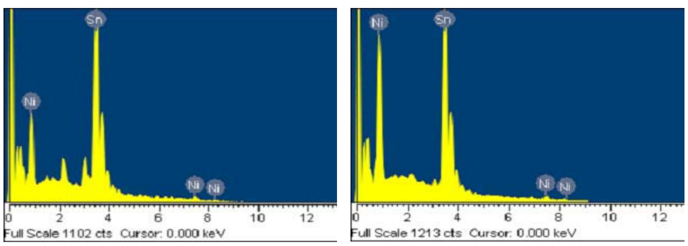

(a) (b)

Fig. 5: EDX analysis for morphology and the composition of the intermetallic compound, (a) Sn-Ag solder and (b) Sn-Pb solder

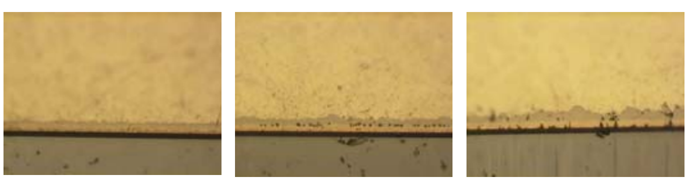

Sn-Ag solder for 24 hours | Sn-Ag solder for 480 hours | Sn-Ag solder for 1000 hours

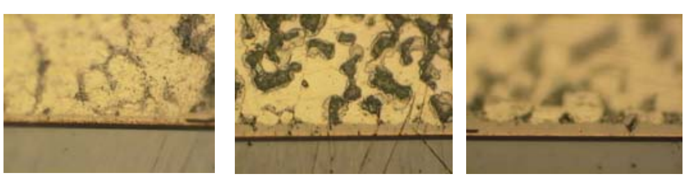

Sn-Pb solder for 24 hours | Sn-Pb solder for 480 hours | Sn-Pb solder for 1000 hours

Fig. 6: The intermetallic compound layers of test vehicles of Sn-Ag and Sn-Pb systems

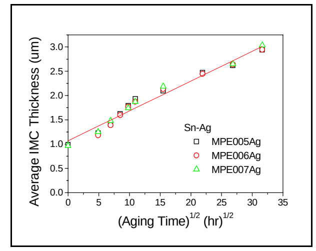

(a)

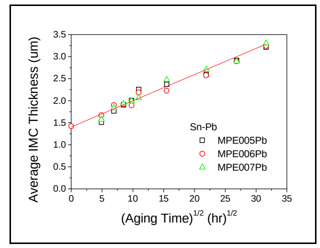

(b)

Fig. 7: The average thickness of intermetallic compound layer (Ni_3Sn_4) versus (aging time)$^{1/2}$ in (a) Sn-Ag and (b) Sn-Pb solders

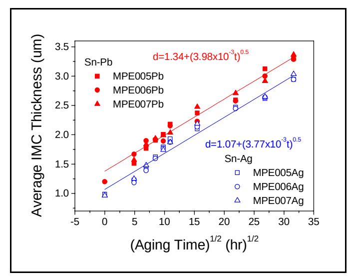

Fig. 8: A comparison of the intermetallic compound growth rate versus (aging time)$^{1/2}$ between the Sn-Ag and Sn-Pb solders

Figure 8 reveals a comparison of the intermetallic compound growth rate versus (aging time)$^{1/2}$ between the Sn-Ag and Sn-Pb solder systems. It is observed that for both Sn-Ag and Sn-Pb solder systems, the intermetallic compound thickens roughly as $t^{1/2}$ in a linear manner, where t is the aging time as expected for diffusion-controlled growth. An equation of diffusion coefficient (as shown in equation 1) has been used to model the isothermal growth kinetics of the intermetallic layer thickness.

$$d = d_0 + (Dt)^{1/2} \quad (1)$$

Where d is the total thickness of the intermetallic compounds growth, d_0 is the initial thickness of the intermetallic compounds layer, D is the diffusion coefficient (or the growth rate of the intermetallic compounds layer), t is the isothermal aging time. From Eq.1, the isothermal growth of intermetallic layer of Sn-Ag and Sn-Pb solder can be expressed as following:

$$d_{Sn/Pb} = 1.34 + (3.98x10^{-3}t)^{1/2} \quad (2)$$

$$d_{Sn/Ag} = 1.07 + (3.77x10^{-3}t)^{1/2} \quad (3)$$

Where Eq.2 and Eq.3 indicates the isothermal growth of intermetallic layer of Sn-Pb and Sn-Ag solder, respectively. It is found that in Eq.2 and Eq.3, the intermetallic compound growth rate of the Sn-Pb solder system is higher than that of the Sn-Ag one (the diffusion coefficients of Sn-Pb and Sn-Ag solder are 3.98×10^{-3} and 3.77×10^{-3}, respectively). This result indicates that the UBM/Sn-Ag solder bump systems utilized in this research do indeed display a good diffusion barrier to retard the formation of intermetallic compound between UBM and solder interface. In addition, it can be seen in figures 6 and 7 that there is no significant variation of intermetallic compound growth rate between different solder volume and UBM size, for both lead-free and lead-containing solder materials. These intermetallic compound growth phenomena can be profitable information for realizing the mechanical behavior of solder bumps after isothermal aging.

- Effects of isothermal aging on solder bump strength

In this study, a shear test was conducted on six test vehicles: MPE005Pb, MPE006Pb, MPE007Pb, MPE005Ag, MPE006Ag and MPE007Ag to determine the solder bump strength after isothermal aging. In this section, four topics are discussed: the effect of the shear speed on the solder bump shear test, the effect of the solder bump dimension on the solder bump strength, the comparison of the bump strength between Sn-Ag and Sn-Pb solders, and the relationship between solder bump strength and intermetallic compound growth rate.

A. The effect of the shear speed on the solder bump shear test

Figure 9 indicates the bump strength variation of Sn-Ag and Sn-Pb solders versus the isothermal aging time under different shear speeds.

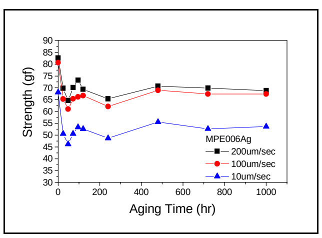

(a) MPE006Ag

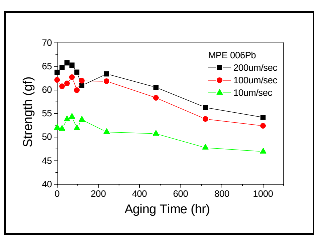

(b) MPE006Pb

Fig. 9: The bump strength variation of Sn-Ag and Sn-Pb solders versus the isothermal aging time under different shear speeds, (a) Sn-Ag solder and (b) Sn-Pb solder

Figure 9 reveals that the bump strength varies with the shear speed, a higher shear speed implies a higher shear strength. It is worth noting that within these three testing speeds, the speed of 10μm/sec reveals the lowest solder strength, followed by the speed of 100μm/sec and then, the speed of 200μm/sec which shows the highest solder bump strength. However, there is little difference in solder bump strength between the 100μm/sec speed and the 200μm/sec speed. Since the strength will remain constant for time-independent deformation, the loss in strength of the solder bump for a reduced shear rate can be attributed to the creep mechanism. The high loading rate strongly promotes the linear-elastic behavior and increases the tendency of brittleness in the material. At faster loading rates, the shear strength increases since time becomes too short for the nucleation and motion of the dislocations. Similarly, in faster tests the dominant crack in the brittle solids does not have the time to grow to its critical size, which can be observed in slower speed tests. The lack of dislocation activity is believed to be responsible for the high shear strength at higher shear speed.

On the other hand, in Fig. 9 it can also be observed that the trends of the solder bump strength degradation after isothermal aging is not altered by different shear speeds. Based on this experimental result, it is noted that the shear test should be a qualitative analysis for the solder bump strength determination rather than a quantitative one. To conclude, both Sn-Ag and Sn-Pb solders show a similar mechanism to the shear speed effect.

B. The solder bump dimension effect on the bump strength

Figure 10 illustrates the bump strength variation of Sn-Ag and Sn-Pb solders versus the isothermal aging time under different solder bump dimensions.

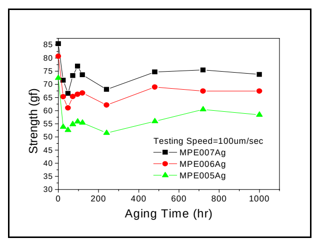

(a) Sn-Ag solder

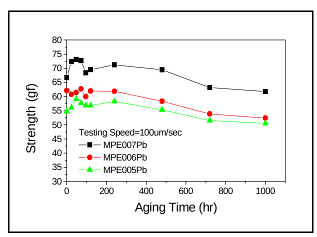

(b) Sn-Pb solder

Fig. 10: The bump strength variation of Sn-Ag and Sn-Pb solders versus the isothermal aging time under different solder bump dimensions, (a) Sn-Ag solder and (b) Sn-Pb solder

It can be seen in figure 10 that for both Sn-Ag and Sn-Pb solders, the test vehicle of MPE007 shows the highest solder bump strength, followed by MPE006, MPE005 shows the lowest solder bump strength. As listed in table 1, the UBM diameters of MPE007, MPE006 and MPE005 are 130μm, 120μm and 110μm, respectively. Therefore it can be concluded that the larger the UBM size the higher the solder strength is. Although different UBM size causes different solder bump strength, the trend of the intermetallic compound formation affecting the solder bump strength are similar.

C. The comparison of the bump strength between Sn-Ag and Sn-Pb solders

Figure 11 indicates the solder bump strength comparison between Sn-Ag and Sn-Pb systems in relation to isothermal aging time.

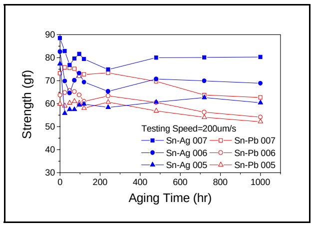

(a) At shear speed of 200 μ m/sec

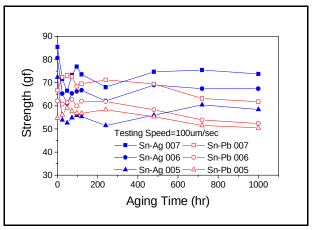

(b) At shear speed of 100 μ m/sec

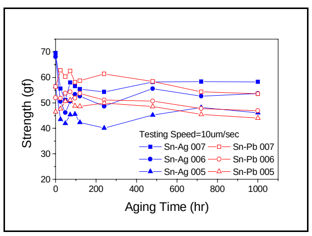

(c) At shear speed of 10 μ m/sec

Fig. 11: The solder bump strength comparison between Sn-Ag and Sn-Pb systems versus isothermal aging time

The figures show that for both Sn-Ag and Sn-Pb solder systems, although the absolute shear strength shows some variation, the different shear speed and different solder bump dimension are similar in behavior when it comes to the shear strength for all the test vehicles, which corresponds with the detailed mechanisms mentioned in the former sections.

The Sn-Ag solder has an average bump strength degradation of 20% after 24 hours isothermal aging. Subsequently, during the aging time of 48 hours to 500 hours, the shear strength of the Sn-Ag solder bump upgrades and degrades, which shows an unstable variation. However, after 500 hours, it reveals relatively stable bump shear strength over the whole duration of aging time. The total shear strength degradation after 1000 hours is about 15% for the Sn-Ag alloy. On the other hand, the Sn-Pb solder has a slight bump strength increase of 8% after 24 hours isothermal aging. Subsequently, the shear strength of the Sn-Pb solder bump shows an unstable variation during the aging time of 48 hours to 240 hours. Finally, the bump shear strength degrades gradually over the remaining duration of the aging time. The total shear strength degradation is estimated at about 15% for the Sn-Pb alloy. One can see that the Sn-Ag solder bump shows unstable shear strength than the Sn-Pb solder for the first 500 hours of aging time. This is due to the fact that an "interlock" effect occurs inside the Sn-Ag solder bump/Ni_3Sn_4 interface. The interface of the intermetallic compound layer and the Sn-Ag solder bump are observed as a rougher surface (as shown in Fig. 4) which will influence the bump shear strength. From these results, it can be observed that the total shear strength degradations of the Sn-Ag and Sn-Pb solder bumps after 1000 hours are similar, however, the Sn-Ag solder shows a better bump strength maintenance (as shown in Fig. 11). Also, the Sn-Ag solder basically could provide a higher bump strength of about 25%, therefore it can be said that it offers a higher intermetallic compound effect resistance during high temperature storage as compared to the Sn-Pb solder.

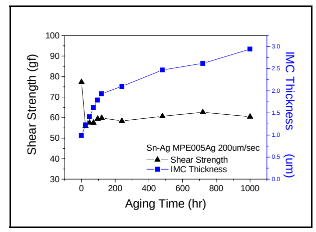

(a) MPE005Ag

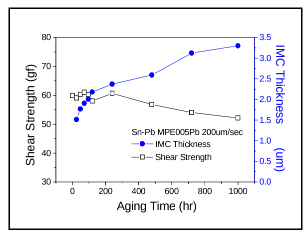

(b) MPE005Pb

Fig. 12: The relationship between solder bump strength and intermetallic compound layer thickness after aging, (s)Sn-Ag solder and (b) Sn-Pb solder

A flip chip design rule indicates that the bump shear strength must exceed 3.1mg/μm^2 [16]. Equation 4 gives the minimum bump shear force:

$$F_{bf}=F_{bs} \times A \tag{4}$$

Where F_{bf} is the minimum bump shear force, F_{bs} is the bump shear strength in the design rule, and A represents the UBM area and equals π x (UBM radius)^2 for a round shaped UBM. Therefore, in this investigation, the minimum requirement bump shear force can be calculated as: MPE005: 3.1mg/μm^2 x π x (55μm)^2 = 29.46g, MPE006: 3.1mg/μm^2 x π x (60μm)^2 = 35.06g and MPE007: 3.1mg/μm^2 x π x (65μm)^2 = 41.15g. Comparing this design rule with the bump shear strength during 1000 hours isothermal aging for both Sn-Ag and Sn-Pb solders, it is found that all test vehicles can transcend this basic design rule. Furthermore, the fracture surface inspections also indicate that the failure of the solder bumps under shear testing are located at the intermetallic compound layer or inside the solder bump. This confirms that the selected Ti/Cu/Ni UBMs on the Cu chip is feasible for the electroplating Sn-Ag solder bumping process.

D. The relationship between solder bump strength and the intermetallic compound growth rate

One factor affecting the solder bump strength during isothermal aging is the intermetallic compound layer thickness. Figure 12 depicts the relationship between solder bump strength and intermetallic compound layer thickness after thermal aging.

In figure 12, the Sn-Pb solder reveals a growth rate higher than that of the Sn-Ag solder, this phenomenon can be one of an important factor that the Sn-Pb solder provides a weaker bump strength maintenance than that of the Sn-Ag solder.

Effects of isothermal aging on the fracture surface

Both Sn-Ag and Sn-Pb solders failed inside the solder bump after 1000 hours isothermal aging. This phenomenon implies that the selected Ti-Cu-Ni UBM layer is favorable for both solder alloys.

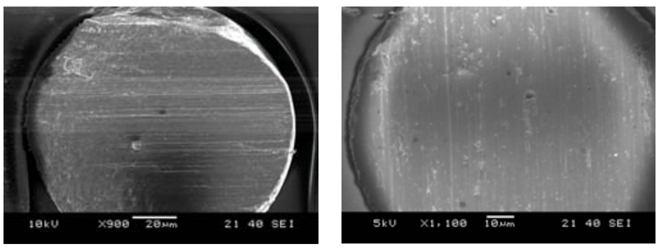

(a) As-reflowed (b) Aging 1000 hours

Fig. 13: The fracture surface of the Sn-Ag solder at (a) as-reflowed and (b) 1000 hours

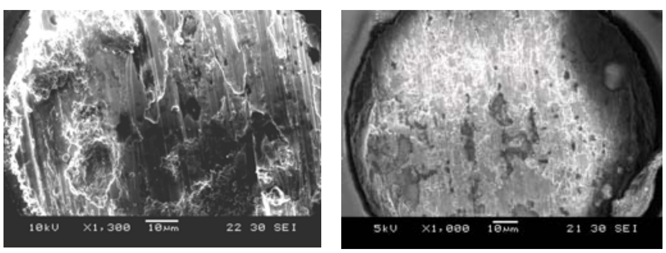

(a) As-reflowed (b) Aging 1000 hours

Fig. 14: The fracture surface of the Sn-Pb solder at (a) as-reflowed and (b) 1000 hours

Figures 13 and 14 show the fracture surface of the Sn-Ag and Sn-Pb solder, as-reflowed as well as at 1000 hours isothermal aging time. It can be observed in figure 15 that as-reflowed, the fracture surfaces are rough as well as lumpy, and exhibit vast amounts of plastic deformation within the Sn-Pb solder bumps. In figure 13(a), the fracture surface of Sn-Ag solder also shows plastic deformation, however, the lumpy area on the fracture surface of Sn-Ag solder is much less than on the Sn-Pb one. As the aging time increases, the fracture mode varies. In figures 13(b) and 14(b), both the Sn-Ag and Sn-Pb systems display a large percentage of brittle fracture surfaces with the increase in isothermal aging time. When comparing the fracture surface of the Sn-Ag and Sn-Pb solders, it is found that the fracture surfaces of the Sn-Pb solder show an obvious difference between the as-reflowed and 1000 hours aging conditions. In contrast, the fracture surfaces of the Sn-Ag solder depict an unapparent variation between conditions of as-reflowed and 1000 hours aging. A grain of Ni/Sn compound was confirmed by EDX on the fracture surface. This demonstrates that the intermetallic compound formation can certainly affect the solder bump mechanical behavior. On the other hand, after 1000 hours aging, the fracture mode of the Sn-Ag and Sn-Pb solders shows some difference. The Sn-Ag solder reveals an almost total-brittle fracture surface, however, the Sn-Pb solder also shows some ductile fracture surface. This could be explained by a specific phenomenon: the Pb-rich area of the Sn-Pb solders diffuses toward the UBM/solder interface as the isothermal aging time increases, as is shown in figure 15. Nevertheless, the composition of the Sn-Ag solder does not reveal this phenomenon. A Pb-rich phase will cause a ductile fracture interface, and the solder with enriched Pb implies a lower shear property [2]. Evidence is shown in figure 13(b) The spots on the fracture surface are found to be Pb-rich areas (confirmed by EDX), which implies that the fracture may happen in both the Pb-rich area and the Ni/Sn intermetallic compound layer. That indicates that the diffusion of the Pb towards the UBM/solder interface after aging will degrade the solder strength. This could explain why the fracture surface of the Sn-Ag solder is more brittle than that of the Sn-Pb solder, and why the solder strength of Sn-Ag solder shows a better maintenance than that of Sn-Pb solder.

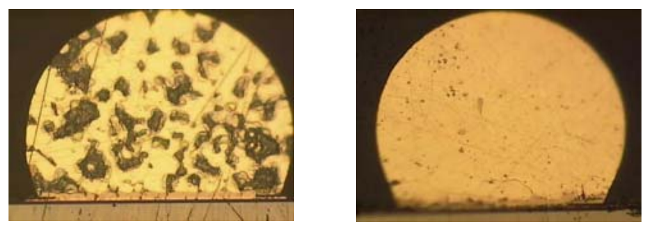

(a) (b)

Fig. 15: The Pb-rich area of the Sn-Pb solders diffuse to the UBM/solder interface, (a) Sn-Pb solder and (b) Sn/Ag solder

Effect of intermetallic compound growth rate on solder bump volume and UBM size

From figures 7 and 8, the solder bump volume and the UBM size indicate no significant effect on the intermetallic compound growth rate. This could be explained by the diffusion-controlled nature of the solid-state growth of the interfacial Ni-Sn IMC layer. If its growth is a reaction-controlled process, then the total number of reactions between Ni and Sn, and hence the time required to form a unit thickness of interfacial Ni-Sn IMC is greater for a large pad size. However, this is not the case in the present study. This observation further confirms the diffusion-controlled nature of solid-state growth of interfacial Ni-Sn IMC in electroplated flip chip solder bumps.

In contrast, figure 10 displays that the solder volume and the UBM size play an important role in the solder bump strength for both Sn-Ag and Sn-Pb solder systems. Therefore, the designer can increase the solder volume and the UBM size to enhance the solder bump strength, and not have to worry about an increase of the intermetallic compound growth rate.

V. Conclusions

In accordance with the results of this investigation, the following conclusions were made. The study of shear displacement rate effect on the solder bump strength indicates that the analysis of bump strength versus thermal aging time should be identified as a qualitative analysis for solder bump strength determination rather than a quantitative one. In terms of the solder bump volume and the UBM size effects, the larger the UBM size the higher the solder bumps shear strength, while at the same time, there is no significant influence on intermetallic compound formation mechanism for both lead-containing and lead-free materials. In addition, the UBM size and solder volume show no distinct difference in the trend of strength degradation of solder bumps in the duration of isothermal aging. The bump shear test findings also show that after 150^{o}C isothermal aging treatment over 1000 hours, the Sn-Ag solder reveals a better bump strength maintenance and a lower intermetallic compounds growth rate than that of Sn-Pb solder. Furthermore, the test vehicles of copper chip with the selected Titanium/Copper/Nickel UBMs shows good bump strength after 150 ^{o}C isothermal aging for 1000 hours, in both electroplated Sn-Ag and Sn-Pb solder bumps. Based on these results, it is confirmed that the selected UBMs on the copper chip is feasible for the electroplating Sn-Ag solder bumping process.

Acknowledgments

The authors would like to thank the VIA Technology Corporation for providing the financial support for this research.

References

1. J.K Lin, A.D Silva, D. Frear, Y.F Guo, J,W Jang, L. Li, D. Mitchell, B. Yeung and C. Zhang, “Characterization of Lead-Free Solders and Under Bump Metallurgies for Flip-Chip Package”, IEEE Transactions on Electronics Packaging Manufacturing, Vol. 25, No. 3, July 2002, pp. 300-307.
2. Ming Li, K.Y Lee, D.R. Olsen and William T. Chen, Ben Tin Chong Tan, and Subodh Mhaisalkar, ”Microstructure, Joint Strength and Failure Mechanism of SnPb, and Pb-Free solders in BGA Packages”, IEEE Transactions on Electronics Packaging, Vol.25, No.3, July 2002, pp. 185-192
3. Se-Young Jang, Juergen Wolf, Oswin Ehrmann, Heinz Gloor, Herbert Reichl, and Kyung-Wook Paik, “Pb-Free Sn/3.5Ag Electroplating Bumping Process and Under Bump Metallization (UBM)”, IEEE Transactions on Electronics Packaging Manufacturing, Vol. 25, No. 3, July 2002, pp. 193-202
4. Hirokazu Ezawa, Masahiro Miyata, Soichi Honma, Hiroaki Inoue, Tsuyoshi Tokuoka, Junichiro Yoshioka, and Manabu Tsujimura, “Eutectic Sn–Ag Solder Bump Process for ULSI Flip Chip Technology”, IEEE Transactions on Electronics Packaging Manufacturing, Vol. 24, No. 4, October 2001, pp. 275-281.
5. N. S. Kim, S. Y. Jung and S. Y. Oh, “Reliability of the Pb-free Solder Bump on Electroless Ni Under Bump Metallurgies”, Electronic Components and Technology Conference, 2003, pp. 77-82.
6. Jae-Woong Nah and Kyung-Wook Paik, “Investigation of Flip Chip Under Bump Metallization Systems of Cu Pads”, IEEE Transactions on Components and Packaging Technologies, Vol. 25, No. 1, March 2002, pp. 32-37.
7. K.L. Lin and K.T. Hsu, “Manufacturing and Materials Properties of Ti/Cu/Electroless Ni/Solder Bump on Si”, IEEE Transactions on Components and Packaging Technologies, Vol. 23, No. 4, December 2000, pp. 657-660.
8. Y.Y. Wei and J.G. Duh, “Effect of Thermal Ageing on (Sn-Ag, Sn-Ag-Zn)/PtAg, Cu/Al2O3 Solder Joints”, Journal of Materials Science: Materials in Electronics, 9, 1998, pp. 373-381.
9. K. Zeng, V. Vuorinen and J. K. Kivilahti, “Intermetallic Reactions between Lead-Free Sn-Ag-Cu Solder and Ni(P)/Au Surface Finish on PWBs”, Electronic Components and Technology Conference, 2001.
10. Guo-Wei Xiao, Philip C. H. Chan, Annette Teng, Jian Cai, and Matthew M. F. Yuen, “Effect of Cu Stud Microstructure and Electroplating Process on Intermetallic Compounds Growth and Reliability of Flip-Chip Solder Bump”, IEEE Transactions on Components and Packaging Technologies, Vol. 24, No. 4, December 2001, pp. 682-690.
11. B. Salam, N.N. Ekere and D. Rajkumar, “Study of the Interface Microstructure of Sn-Ag-Cu Lead-Free Solders and the effect of solder Volume on Intermetallic Layer Formation”, Electronic Components and Technology Conference, 2001.
12. Mawer, Andrew J., “BGA Solder Ball Shear Strength,” SUNY-Binghamton-Sixth Annual Electronics Packaging Symposium, July 14, 1995.
13. Richard J. Coyle, and Patrick P. Solan, “The Influence of Test Parameters and Package Design Features on Ball Shear Test Requirements”, IEEE/CPMT Int’l Electronics Manufacturing Technology Symposium, 2000, pp. 168-177.
14. S. K. Kang, R. S. Rai, and S. Purushothaman, “Interfacial Reactions During Soldering with Lead–Tin Eutectic and Lead (Pb)-Free, Tin-Rich Solders”, Journal of Electronic Material, Vol. 25, No. 7, 1996, pp. 1113.
15. S. Choi, T. R. Bieler, J. P. Lucas, and K. N. Subramanian, “Characterization of the Growth of Intermetallic Interfacial Layers of Sn–Ag and Sn–Pb Eutectic Solders and Their Composite Solders on Cu Substrate During Isothermal Long-Term Aging”, Journal of Electronic Material, Vol. 28, No. 11, 1999, pp. 1209.
16. K.M Chen and K.N. Chiang, “Impact of Probing Procedure on Flip Chip Reliability”, Journal of Microelectronics Reliability, Vol. 43, January, 2003, pp. 123-130.